

Urban Stormwater Drainage Design: Integration of Conventional and Sustainable Technologies in Puerto Villamil, Galápagos

Diseño de Alcantarillado Pluvial Urbano: Integración de Tecnologías Convencionales y Sostenibles en Puerto Villamil, Galápagos

Giancarlo Bravo*
Karla Bravo*
Clemencia Coello*

ABSTRACT

Isabela Island faces stormwater management challenges due to its topography and extreme weather events. This study was conducted to design an efficient and sustainable stormwater drainage system for Puerto Villamil, with the aim of preventing sanitary sewer system overload and reducing environmental impact. The design was developed using hydraulic calculations in spreadsheets, validated with SWMM software, and took into account technical standards and local conditions. Nature-based solutions such as permeable pavements, tree pits, and rain gardens were incorporated. The final design included 136 pipes, 136 manholes, and 3 outfalls, with 2.12 ha allocated to Sustainable Urban Drainage Systems (SUDs). Runoff volume was reduced by 38%, and pipe diameters and excavation volumes were optimized. The project represents an innovative alternative for water management in protected areas, aligned with SDGs 6, 11, and 14.

Keywords: Stormwater drainage, runoff, sustainability, hydraulic design, SUDs.

* Eng. Escuela Superior Politécnica del litoral, Guayaquil Ecuador, bravo@espol.edu.ec, <https://orcid.org/0009-0004-8192-245X>

* Arch. Quevedo State Technical University, kbravoc5@uteq.edu.ec, <https://orcid.org/0000-0003-3253-187X>

* Ph.D. Quevedo State Technical University, Ccoello@uteq.edu.ec <https://orcid.org/0000-0002-6251-9233>

JOURNAL OF BUSINESS
and entrepreneurial
studies

ISSN: 2576-0971



Atribución/Reconocimiento-NoComercial- Compartir Igual 4.0 Licencia Pública Internacional — CC

BY-NC-SA 4.0

<https://creativecommons.org/licenses/by-nc-sa/4.0/legalcode.es>

Journal of Business and entrepreneurial
April - June Vol. 10 - 2 - 2026
<http://journalbusinesses.com/index.php/revista>
e-ISSN: 2576-0971
journalbusinessentrepreneurial@gmail.com
Receipt: 19 November 2025
Approval: 12 January 2026
Page 1-32

RESUMEN

La Isla Isabela, enfrenta problemas de gestión pluvial debido a su topografía y eventos climáticos extremos. Este trabajo se realizó para diseñar un sistema de alcantarillado pluvial eficiente y sostenible para Puerto Villamil, con el fin de evitar la saturación del alcantarillado sanitario y reducir el impacto ambiental. El diseño se elaboró mediante diseños hidráulicos en hojas de cálculo, validados con el software SWMM, considerando normas técnicas y condiciones locales. Se incorporaron soluciones basadas en la naturaleza como pavimentos permeables, alcorques y jardines de lluvia. El diseño final incluyó 136 tuberías, 136 pozos y 3 descargas, con una asignación de 2,12 ha a Sistemas Urbanos de Drenaje Sostenible (SUDs). Donde se redujo 38% el volumen de escorrentía se optimizó diámetros y excavaciones. El proyecto representa una alternativa innovadora para la gestión del agua en zonas protegidas, alineada con los ODS 6, 11 y 14.

Palabras clave: Alcantarillado pluvial, escorrentía, sostenibilidad, diseño hidráulico, SUDs.

INTRODUCTION

Stormwater management is essential in urban environments due to the challenges posed by runoff. Uncontrolled accumulation of rainwater can cause significant impacts on ecosystems, including flooding, sewer system saturation, soil erosion, and water body contamination (Kravchenko et al., 2024a).

Globally, in areas with high anthropogenic activity, stormwater infiltration can introduce a variety of contaminants into underground aquifers, such as nutrients, heavy metals, and organic compounds. These contaminants not only accumulate but also interact in the subsurface, forming even more harmful secondary pollutants (Karamoutsou et al., 2024).

The mobilization of toxic substances during the infiltration process can compromise groundwater quality, making the implementation of sustainable urban drainage systems crucial to mitigate these risks and protect both water resources and public health (Dong et al., 2024).

In the context of extreme weather events, sustainable stormwater management becomes even more relevant. It is essential to reduce runoff volume, improve water quality, and provide additional benefits to the quality of urban environments, while promoting biodiversity conservation (Karamoutsou et al., 2024).

Collecting data on precipitation frequency and runoff magnitude enables the analysis of water behavior under different climate scenarios, which is key to designing effective management strategies. Projections of water volumes to be managed help prevent flooding and alleviate pressure on existing drainage systems (Yang et al., 2024).

Advanced tools for generating geographic and hydrological models enable the identification of critical areas for designing more efficient and sustainable systems. This approach, based on reliable data, ensures that the stormwater drainage network is effective, cost-efficient, and resilient to climate and urban changes (Senes et al., 2021).

Data analyzed prior to the design of the stormwater drainage network allows the proposal to be adapted to the specific conditions of each urban area. Knowledge of precipitation, topography, and land use improves the capacity to manage water flow, reducing the risk of flooding and overflows (Allende-Prieto et al., 2018).

The Galápagos Islands, located in the Ecuadorian Pacific Ocean, have a subtropical climate with a wet and a dry season, influenced by the Humboldt Current. The islands are characterized by young volcanic soils with low organic fertility. Geographically, the islands feature a wide variety of habitats due to their volcanic origin. Isabela Island, the largest in the archipelago, stands out for its ecological diversity and active volcanoes such as Sierra Negra and Alcedo. Its rich biodiversity makes it a crucial focus for conservation, facing challenges such as mass tourism and invasive species (Maestro, M.; Pérez-Cayeiro, M.L.; Reyes, H.; Chica-Ruiz, J.A., 2024).

Isabela Island has a tropical marine climate with stable temperatures and significant seasonal variations. The rainy season, from December to May, brings frequent rainfall that can affect the sewer infrastructure, while the dry season, from June to November, presents water supply challenges (Alzueta Pérez, 2014). In addition, El Niño and La Niña phenomena introduce interannual variability, influencing precipitation levels and, consequently, resource management and the sustainability of the sewer system. Adaptive planning is crucial for mitigating climate impacts (Burbano, D.V. et al., 2022).

The Isabela Land Use and Development Plan indicates that the existing sanitary sewer system discharges into a deficient pumping station, which becomes overloaded during rains, causing collapses and uncontrolled discharges into water sources such as the Poza de los Flamingos lagoon (Municipal Decentralized Autonomous Government of Isabela, 2023).

Therefore, it is necessary to propose alternative construction solutions to conventional open-trench technology, given the high complexity of the rocky soil. These stormwater management alternatives aim to address surface runoff, the risk of flooding due to waterlogging, and various types of pollution.

The project's objectives include determining baseline data for an alternative and sustainable solution, analyzing various construction alternatives, and developing a detailed design for the stormwater drainage network, including plans, technical specifications, and a budget. This comprehensive approach seeks not only to resolve technical problems but also to protect public health and the environment of Santa Isabela, contributing to the sustainability of the Galápagos Islands.

Stormwater management in urban areas depends on an understanding of key hydrological parameters, such as rainfall intensity, runoff coefficient, and Intensity–Duration–Frequency (IDF) curves, which allow for the estimation of peak flow using the rational method. These fundamentals are essential for designing hydraulic infrastructure that reduces flood risk and optimizes water resource management (Xiao & Vasconcelos, 2023; Diogo & do Carmo, 2019).

In recent decades, urban water management has evolved toward more sustainable approaches, such as Sustainable Urban Drainage Systems (SUDS), which integrate nature-based solutions—permeable pavements, rain gardens, and vegetated swales—to reduce runoff and improve water quality. International experiences, such as sponge cities in China, demonstrate reductions of up to 90% in runoff volume through hybrid strategies that combine green and gray infrastructure (Grigg, 2024; Wang et al., 2024; Zhang et al., 2021).

Various studies in Latin America and Europe have shown that combining conventional systems with sustainable solutions improves hydraulic efficiency and resilience to extreme rainfall. In Brazil and Costa Rica, the implementation of hybrid bio-retention and underground storage systems has significantly reduced surface runoff, demonstrating the applicability of SUDS in tropical contexts (Bouarafa et al., 2019; Chapa et al., 2020).

Among the most effective technologies are permeable pavements, which allow for infiltration and aquifer recharge; structural tree pits, which combine vegetation and contaminant retention; and rain gardens, which reduce nutrients and suspended solids in urban water. These solutions provide not only hydrological benefits but also environmental and social ones, such as improved landscape and urban health (Hu et al., 2018; Lim et al., 2021; Jeon et al., 2021).

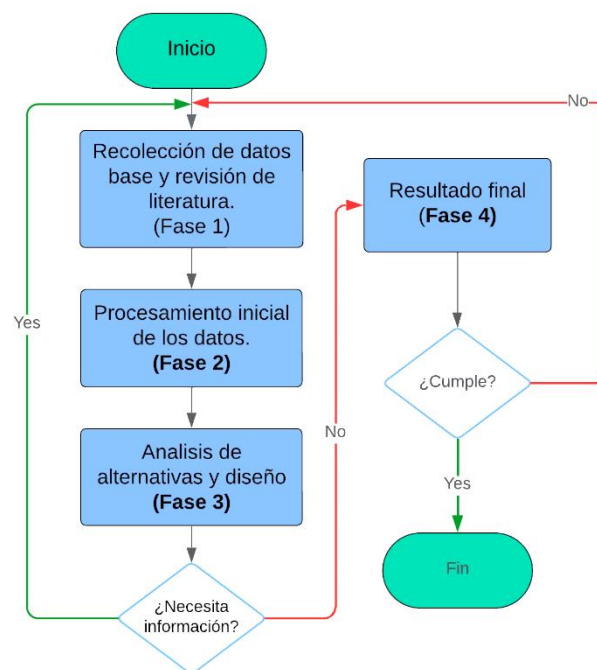
Urban drainage design requires integrating hydrological and hydraulic aspects with economic viability criteria, considering both capital (CAPEX) and operating (OPEX) costs. Recent studies show that, although SUDS may have a higher initial cost, they offer significant long-term returns by reducing maintenance expenses and flood damage (García-Haba et al., 2023; Sulis et al., 2024).

Finally, in the Ecuadorian context, regulations for the Galápagos promote the incorporation of sustainable urban drainage technologies, prioritizing environmental protection and resilience to climate change. This regulatory framework provides a basis for the design of infrastructure adapted to island and sensitive environments (Ragazzi et al., 2016; Francisco et al., 2023)

MATERIALS AND METHODS

The methodology employed in this project follows a Traditional or Sequential approach, where each stage of the process is carried out in a sequential and orderly manner. The flowchart is shown below in Figure 2.6 :

Figure 2 Flowchart of the project methodology [Author's own work]



Phase 1: Data Collection and Meteorological Analysis.

The first phase of the project begins with a comprehensive review of the existing literature on stormwater drainage system design to establish a solid theoretical framework. Next, meteorological and topographic data crucial for the design of the stormwater drainage system in Santa Isabela are collected. This includes gathering data that serves as a foundation for the project, as well as an initial assessment of the problem.

Phase 2: Hydrological Design.

In this phase, the design flow rates necessary to handle the expected water volume during rainfall events are calculated. Using the previously collected meteorological and topographical information, the characteristics of water flow on

the island are analyzed to ensure that the stormwater drainage system is capable of effectively managing runoff. Additionally, the micro-watershed, water flow direction, and land use are defined, taking into account the terrain characteristics to optimize the system design. This comprehensive assessment allows the design to be adapted to the specific conditions of Santa Isabela, ensuring efficient stormwater management and the prevention of flooding problems.

Phase 3: Evaluation of Alternatives and Design.

For this phase, comparative analyses are conducted to identify which of the proposed alternatives best optimizes stormwater management, considering technical, economic, environmental, and social factors. Based on the data obtained in the previous phases, the selected alternative for the stormwater drainage system is designed, evaluating its hydraulic efficiency and its adaptation to the terrain.

Phase 4: Documentation

Finally, the unit price analysis (UPAs), the detailed budget, and the costed project schedule are prepared. In addition, the corresponding technical specifications and detailed drawings of the storm sewer system are prepared, including the final design of the structures and their layout on-site.

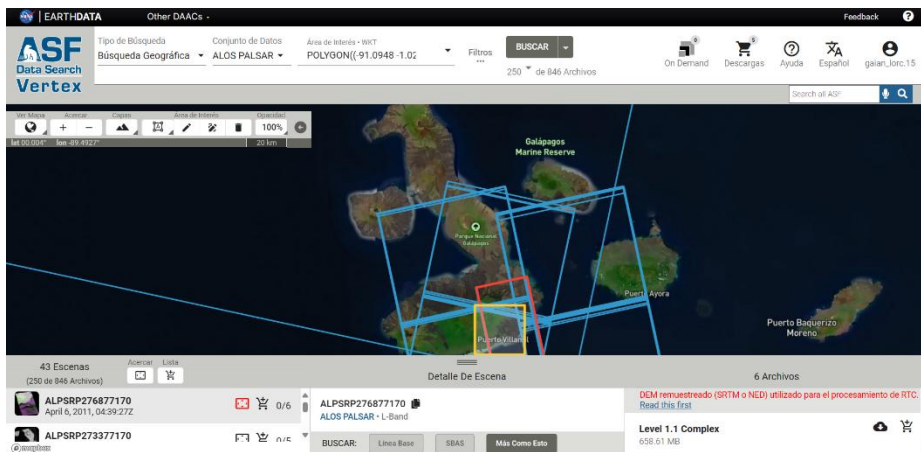
The laboratory or desk work will involve processing the collected data and analyzing it for the design of the stormwater drainage system:

Meteorological Data Analysis: For the analysis of meteorological data, INAMHI's IDF curves for San Cristóbal will be used due to the lack of specific data for Santa Isabela. Although San Cristóbal and Santa Isabela are separate islands, they share similar climatic and meteorological conditions due to their geographical proximity within the Galápagos Archipelago. This similarity in precipitation patterns makes the San Cristóbal IDF curves a reasonable representation of conditions in Santa Isabela. The absence of specific local meteorological data necessitates the use of the closest available data, and the use of San Cristóbal's IDF curves will allow for an adequate estimation of flood risk, which is crucial for designing an effective drainage system in Santa Isabela. In previous studies, the application of meteorological data from a neighboring island has proven to be sufficiently accurate for the planning and design of drainage systems in the region.

Topographic Data Study: The digital terrain models (DTMs) provided by GAD Isabela, along with NASA's Digital Elevation Models (DEMs) Figure 2.7 , were used to obtain high-precision topographic data for the study area. These data were essential for generating surfaces and defining the drainage area. They were analyzed to calculate the catchment area, perform terrain slope calculations, and

verify the accuracy of the topographic measurements. Additionally, these models made it possible to determine runoff areas and analyze water behavior during rainfall events, which was key to the design of the stormwater drainage system.

Figure 3. Earth Data Platform, topographic data extraction [NASA Alaska Satellite Facility, 2024]



Design period: For the Table 2.1 , the design period must be selected taking into account the type of system and the drainage area, as these factors are fundamental to ensuring the system’s durability and efficiency. Considering these variables ensures that the system is adequately adapted to water management conditions and expected extreme events.

Table 1.
 Design periods according to [INEN, 1997]

System Type	Pipe Type	Drainage area	T return [years]
Micro-drainage	Residential, commercial	≤2	2–5
	Pipes in any area	>10	10
	Pipes in any area	>10	10
Macro drainage	Concrete channels and vegetation	≤1000	10–25
	Concrete channels	>1000	10
	Mixed concrete and vegetation channels		50
	Channels including the free edge		100

Land Use Analysis Using ESA Software: Software from the European Space Agency (ESA) was used to obtain detailed information on land use in the study area. These data were used to determine the runoff coefficient, a fundamental parameter in the design of stormwater drainage systems. **Runoff Coefficient:** The EMAAP-Q (2009) runoff coefficient table was used to determine the appropriate values based on surface characteristics and return period.

Hydraulic Equations: Hydraulic equations were used to determine the behavior of water flow in a pipe section. The data were obtained from the technical literature, specifically from the work of López Cualla (2000).

Velocity Ranges and Roughness Coefficient: CPE INEN 9-1 establishes that the velocity in the pipe must not be less than 0.45 m/s to prevent the retention of solids, and a velocity of 0.60 m/s is recommended.

Shear Stress: The self-cleaning condition must be verified for each section of the network, where the average shear stress must be at least 1 Pa, according to EMAAP-Q (2009).

The information collected in the previous phases of the project will be tabulated for analysis and subsequent application in the design of the stormwater drainage system.

IDF Curves: The Intensity-Duration-Frequency (IDF) curves for San Cristóbal, will be used as the basis for flow calculations. This data will be tabulated to show the different rainfall intensities according to the return period and the duration of the rainfall event.

Topographic data: Digital elevation models (DEM) and terrain slope data will be used for processing in geographic information systems. These data will enable the delineation of micro-watersheds and the identification of runoff areas. **Runoff coefficients:** The runoff coefficients to be used will be tabulated and land uses will be plotted

Table 2 .
Runoff coefficient values [EMAAP-Q, 2009]

VALUES USED TO DETERMINE A RUNOFF COEFFICIENT BASED ON SURFACE CHARACTERISTICS

Area Description	Return Period (years)		
	2	5	10
Asphalt	0.73	0.77	0.81
Concrete / Roof	0.75	0.8	0.83
Green areas (gardens, parks, etc.), 50% of the area covered with grass			
- Slope 0–2%	0.32	0.34	0.37
- Average 2–7%	0.37	0.4	0.43
- Grade greater than 7%	0.40	0.43	0.45
Grasslands			
- Flat 0–2%	0.25	0.28	0.3
- Average 2–7%	0.33	0.36	0.38
- Grade greater than 7%	0.37	0.4	0.42

Hydraulic parameters: The hydraulic relationships and maximum velocities will be presented in tables to ensure that the system meets the necessary hydraulic criteria to prevent problems such as sediment accumulation in the pipes.

	$\left(\frac{Q_{Dis}}{Q_o}\right)_r$	$\left(\frac{V}{V_o}\right)_r$	$\left(\frac{d}{D}\right)_r$	$\left(\frac{R}{R_o}\right)_r$	$\left(\frac{H}{D}\right)_r$
0.01		0.292	0.092	0.239	0.041
0.02		0.352	0.124	0.315	0.067
0.03		0.040	0.148	0.370	0.086
0.04		0.427	0.165	0.410	0.102
0.05		0.453	0.182	0.449	0.116
0.06		0.473	0.196	0.481	0.128
0.07		0.492	0.210	0.510	0.140
0.08		0.505	0.220	0.530	0.151
0.09		0.520	0.232	0.554	0.161
0.10		0.540	0.248	0.586	0.170
0.11		0.553	0.258	0.606	0.179
0.12		0.570	0.270	0.630	0.188
0.13		0.580	0.280	0.650	0.197

0.14	0.590	0.289	0.668	0.213
0.15	0.600	0.298	0.686	0.213

RESULTS

This section details the layout of the traditional sewer system and the area where sustainable drainage systems (SUDs) will be implemented in Puerto Villamil, as shown in the Figure3.1 . The layout of the pipes will be based on the local topography, using the following criteria:

Installation depth: The minimum depth will be 1.2 meters; installation at a shallower depth may be considered in certain areas using appropriate backfill. Efforts will be made not to exceed 4 meters to control costs.

Minimum slope: A minimum slope of 0.5% will be established to ensure efficient stormwater flow.

Runoff coefficient and catchment area per manhole

Using the land use data shown in Figure2.13 and from Table2.2 Runoff coefficient values [EMAAP-Q, 2009] Table2.2 , the runoff coefficients are obtained. For this example, well 17, which feeds into pipe 16, will be used.

Well 17					
Catchment	Area [ha]	Runoff coefficient	Street length [m]	Longitudinal slope [%]	Road width [m]
1	0.131	0.78	70.1	0.3	6
2	0.118	0.78	72.52	0.3	7
3	0.404	0.52	147.31	0.3	7

Table3 .8 Description of Well 17 [Author’s own work]

Travel time

Using the equation1 , the travel time is calculated using an initial velocity of 1.2 m/s.

$$t_r = \frac{L}{60 * v} \tag{1}$$

C0	C4	C6	C8
Contribution	Length	Speed	Time elapsed
243	70.10	1.20	0.97
229	72.52	1.20	1.01
222	147.31	1.20	2.05

Table 3.9 Travel time [Author’s own work]

Concentration time

From Equation 2, the concentration time (t_c) is determined by combining the initial time (t_i) and the travel time (t_r), assuming an initial time of 10 minutes.

$$t_c = t_i + t_r \tag{2}$$

Table 3.10 Concentration time [Author’s own work]

C0	C2	C10	C11
Contribution	Area	Retention period	Intensity
243	0.13	5.00	66.20
229	0.12	5.00	66.13
222	0.40	5.00	64.12

Rainfall intensity

Using the formulas derived from the IDF curves (3 equation), rainfall intensity (I) is calculated assuming a 5-year return period.

C0	C8	C9
Contribution	Time elapsed	Concentration time
243	0.97	10.97
229	1.01	11.01
222	2.05	12.05

$$I = 734.3316 \times T^{0.3077} \times t^{-0.7719} \quad 120min < t < 1440min \tag{4}$$

Table 3.11 Rainfall intensity [Own elaboration]

Design flow

Using the Rational Method equation6 , the design flow (Q_{Dis}) is determined by considering a runoff coefficient (C) that depends on factors such as land cover and slope.

$$Q = \frac{C \times I \times A}{360} \tag{6}$$

C0	C2	C11	C12
Contribution	Area	Intensity	Flow
243	0.13	66.20	18.74
229	0.12	66.13	16.85
222	0.40	64.12	37.69

Table 3.12 Design flow rate [Own work]

Actual depth in the ditch

The actual head in the ditch (y) is calculated using Manning’s simplified formula for ditches, in which the depth value must be solved for, as shown in equation(14

$$Q_s = \frac{0.375 \times y^{\frac{8}{3}} \times Z \times S^{1/2}}{n} \tag{14}$$

C0	C5	C12	C29	C30	C20
Contribution	Flow	Flow	n	Z	and
243	0.003	18.74	0.02	50.00	4.98
229	0.003	16.85	0.02	50.00	4.77
222	0.003	37.69	0.02	50.00	6.38

Table 3.13 Actual tension at the curb [Author’s own work]

Wet width

The wet width (T) is calculated as the product of the depth (y) and the inverse of the cross-slope (Z), using the equation(10 :

$$T = y \times Z \tag{10}$$

C0	C20	C30	C21
Contribution	and	Z	T
243	4.98	50.00	248.79
229	4.77	50.00	238.57
222	6.38	50.00	318.86

Table 3 .14 Wet width [Author's own compilation]

Cross-sectional area

The cross-sectional area (Atransversal) is calculated using the equation11 :

$$A_{transversal} = \frac{y \times T}{2} \tag{11}$$

C0	C12	C23	C22
Flow	Flow	Atrans	V Actual
243	18.74	0.066	0.30
229	16.85	0.061	0.30
222	37.69	0.112	0.37

Table 3.15 Cross-sectional area [Author’s own work]

Flow velocity

The flow velocity (v) is calculated using the relationship between the flow rate (Q) and the cross-sectional area (A), according to the equation(12 :

$$v = \frac{Q}{A} \tag{12}$$

C0	C20	C21	C23
Contribution	and	T	Atrans
243	4.98	248.79	0.066
229	4.77	238.57	0.061
222	6.38	318.86	0.112

Table3 .16 Flow velocity [Author’s own work]

Now, using this calculated velocity, the travel time, residence time, concentration, and flow rate are recalculated.

C0	C24	C25	C26	C27
Contribution	t distance	t concentration	Intensity	Flow
243	3.86	13.86	61.12	17.31
229	4.08	14.08	60.79	15.49
222	6.62	16.62	57.44	33.77

Table 3.17 Values corrected with the new travel speed [Author’s own work]

Control tie

The control tie (yco) is calculated using the ratio of the critical tie (Tco) to the inverse of the cross-slope (Z), using the equation13 :

$$y_c = \frac{T_c}{Z} \tag{13}$$

C0	C30	C37	C38
Contribution	Z	Tco	yco
243	50.00	350.00	7.00
229	50.00	300.00	6.00
222	50.00	350.00	7.00

Table 3.18 Control Tie [Own Work]

Drainage Capacity

The drainage capacity (Qs) in a ditch is determined by applying the14 flow equation based on the Manning coefficient and the geometric and hydraulic parameters:

$$Q_s = \frac{0.375 \times y^{\frac{8}{3}} \times Z \times S^{1/2}}{n} \tag{14}$$

C0	C5	C29	C30	C37	C38	C39
Contribution	Pending	n	Z	Tc	and	Qs
243	0.003	0.02	50.00	350.00	7.00	42.74
229	0.003	0.02	50.00	300.00	6.00	28.33
222	0.003	0.02	50.00	350.00	7.00	42.74

Table3 .19 Drainage capacity [Author's own compilation]

Number of inlets

The number of drains required (N) is determined by dividing the design flow (Qdis) by the drainage capacity of the gutter (Qs), equation15 :

$$N = \frac{Q_{Dis}}{Q_s} \tag{15}$$

C0	C27	C39
Contribution	Flow	Qs
243	17.31	42.74
229	15.49	28.33
222	33.77	42.74

Table 3.20 Number of sumps [Author's own work]

Calculation of pipes and wells

As an example, consider pipe 18, which runs from well 19 to well 20.

Concentration time

The concentration time (tc) is determined by combining the initial time (ti) and the travel time (tr), considering the concentration time of the previous section as the initial time.

C0	C5	C9	C10	C11	C12
Home	Initial	Assumed	Estimated	Calculated	Calculated
Pipe	Length	Velocity	Concentration time		
	L_Pipe	V Test	T initial	T elapsed	Concentration time
	[m]	[m/s]	[min]	[min]	[min]
18	74	2.12	19.7	0.6	20.3

Table3 .22 Initial time, travel time, and concentration time [Author's own work]

Travel time and concentration time

Travel time (tr) is calculated using Equation (1) with an initial velocity of 2.12 m/s obtained in Section 3.1.4.10, and concentration time (tc) is determined as the sum of initial time (ti) and travel time (tr), according to Equation 2.

Rainfall intensity

Rainfall intensity (III) is calculated using the formula derived from the IDF curves, Equation 3.

C0	C10	C11	C12	C13	C14
Initial	Calculated	Calculated	Calculated	Standardized	Calculated
Piping	Concentration time			Coefficient	Rainfall intensity
	Initial T	Travel time	Concentration T	Retention period	
	[min]	[min]	[min]	[Years]	[mm/hr]
18	19.7	0.6	20.3	5	63.7

Table3 .23 Rainfall intensity [Author's own compilation]

Catchment area

The cumulative catchment area (AAcumulada) is calculated by summing the individual areas of each contribution, Equation 5:

$$A_{Acumulada} = A_1 + A_2 + A_3 + \dots + A_n \tag{5}$$

C0	C6	C7
Initial	Home	Initial
Piping	Area	
	Own	Cumulative
	[Ha]	[ha]
18	0.57	21.95

Table 3.24 Catchment Area [Own work]

Discharge

The flow rate (Q) is calculated using the Rational Method formula, Equation6 :

C0	C6	C7	C8	C14	C18
Home	Home	Initial	Standard	Calculated	Calculated
Piping	Area		Coefficient	Rainfall intensity	Flow
	Instantaneous	Cumulative	C (runoff)		without SUDs
	[ha]	[Ha]	[Dimensionless]	[mm/hr]	[L/s]
18	0.57	21.95	0.53	53.7	1742

Table3 .25 Flow [Author’s own work]

Flow infiltrated by the sustainable drainage system

The infiltrated flow (Q_{infil}) is calculated by considering the permeability and area of the sustainable drainage system (SUDs), using the equation7 :

$$Q_{infil} = k * A_{SUDs} \quad (7)$$

C0	C15	C16	C17
Initial	Assumed	Estimated	Calculated
Piping	SUDs		
	Permeability K	SUDs area	Filtered flow
	[m/s]	[ha]	[L/s]
18	0.00010	0.677	676.9

Table3 .26 Infiltration flow through the sustainable drainage system [Author’s own work]

Design flow

The design flow (Q_{Dis}) is calculated by subtracting the infiltrated flow (Q_{infil}) from the flow without SUDs (Q), according to the equation8 :

$$Q_{Dis} = Q - Q_{infil} \quad (8)$$

C0	C17	C18	C19
Initial	Calculated	Calculated	Calculated
Piping	Flow	Flow	Flow
	filtered	without SUDs	Design
	[L/s]	[L/s]	[L/s]
18	676.9	1742.0	1065.2

Table3 .27 Design flow rate [Author’s own work]

Pipe diameter

The required pipe diameter (D_{Dis}) is calculated using Manning’s formula¹⁶ to determine the hydraulic diameter based on the design flow rate (Q_{Dis}), the slope (S), and the roughness coefficient (n).

$$D_{Dis} = 1.548 \left(\frac{n * Q_{Dis}}{\sqrt{S}} \right)^{3/8} \quad (16)$$

C0	C20	C21	C22	C23	C22	C23	C22	C23
Initial	Assumed	Standard	Calculated	Calculated	Calculated	Calculated	Assumed	Assumed
Piping	Slope S [%]	Manning Pipe_Diameter [s/m ^{1/3}]	Required diameter		True required diameter		Commercial Diameter	
			In meters [m]	In inches [in]	Previous sections			
					[m]	[in]	[m]	[in]
18	0.5	0.011	0.805	31.7	34.00	0.860	36	0.91

Table 3.28 Pipe diameter [Own work]

Full-pipe flow

The flow rate (Q_o) is determined under full-pipe conditions, considering the adopted diameter and using Manning’s equation¹⁷:

$$Q_o = 312 * \frac{D_{Dis}^{8/3} * S^{1/2}}{n} \quad (17)$$

C0	C28	C29	C30
Initial	Calculated	Calculated	Calculated
Pipe	Solid pipe		
	Rh ₀	Q ₀	V ₀
	[m]	[L/s]	[m/s]
18	0.23	1480	2.27

Table 3.29 Full-pipe flow (flow rate, hydraulic radius, and velocity) [Author’s own work]

Full-pipe flow rate, full-pipe hydraulic radius, and full-pipe velocity

The maximum full-pipe flow rate (Qo) is calculated using Equation 17, while the full-pipe hydraulic radius is determined using Equation 18 and the full-pipe velocity is obtained from Equation 19.

$$R_{h0} = \frac{D_{Dis}}{4} \tag{18}$$

$$V_o = \frac{R_{h0}^{\frac{2}{3}} * S^{1/2}}{n} \tag{19}$$

Hydraulic relationships

Hydraulic relationships allow parameters such as flow rate, velocity, head, and hydraulic radius to be compared with full-pipe conditions.

C0	C31	C32	C33	C34	C35	C36
Initial	Calculated	Table	Table	Table	Table	Condition
Piping	Hydraulic Ratios					
	Q/Q_0	V/V_0	d/D	R/R_0	H/D	
	[Dimensionless]	[Dimensionless]	[Dimensionless]	[Dimensionless]	[m/s]	Condition
18	0.72	0.955	0.705	1.182	0.67	COMPLIES

Table 3.30 Hydraulic relationships [Author’s own work]

$$\left(\frac{H}{D}\right)_r = 0.67 \leq 0.85$$

Actual flow in the section

C0	C37	C38	C39	C40	C41	C46
Initial	Calculated	Condition	Calculated	Calculated	Calculated	Calculated
Pipe	Velocity		T path 2	Water depth	Hydraulic radius	Hydraulic depth
	V		Corrected	d	R	H
	[m/s]	Condition	[min]	[m]	[m]	[m]
18	2.17	MEETS	0.6	0.64	0.27	0.58

Table 3.31 Actual flow in the section [Own work]

Velocity

The actual flow velocity is calculated by adjusting the full-pipe velocity using the corresponding hydraulic ratio, equation21 . Comparing with the velocity used at the beginning

$$\%error = \left(\frac{2.17 - 2.12}{2.17} \right) = 2.5\% \rightarrow \text{Variación mínima}$$

Water depth, hydraulic radius, and hydraulic depth

The water depth (d) inside the pipe is calculated by multiplying the design diameter (Dis) by the corresponding hydraulic ratio (d/D)_r, equation22 . The hydraulic radius (Rh) is calculated by multiplying the hydraulic radius for a full pipe (Rh0) by the corresponding hydraulic ratio (R/Ro)_r, equation23 . The hydraulic depth (H) is calculated by multiplying the required pipe diameter (DDis) by the corresponding hydraulic ratio (H/D)_r, equation24 .

$$\zeta d = D_{Dis} * \left(\frac{d}{D} \right)_r$$

$$R_h = \frac{D_{Dis}}{4} * \left(\frac{R}{R_o} \right)_r$$

$$H = D_{Dis} * \left(\frac{H}{D} \right)_r$$

Shear stress

The shear stress (τ) is calculated using the equation25 :

$$\tau = \gamma * R_h * S \quad (25)$$

C0	C20	C41	C42	C43
Initial	Assumed	Calculated	Calculated	Condition
Piping	Slope	Hydraulic radius	Stress	
	S	R	Tao	
	[%]	[m]	[N/m ²]	Condition
18	0.5	0.27	11.9	MEETS

Table 3.32 Shear stress [Author’s own work]

Velocity height

The velocity height is calculated using the equation26 :

$$h_v = \frac{v^2}{2 * g} \quad (26)$$

C0	C37	C38	C40
Initial	Calculated	Condition	Calculated
Pipe	Velocity		Velocity head
	V		(V1^2)/(2*g)
	[m/s]	Condition	[m]
18	2.17	MEETS	0.24

Table 3.33 Velocity head [Author’s own work]

Specific energy for actual flow

The specific energy for the actual flow is calculated by adding the water depth (d) and the velocity head (hV), equation27 :

C0	C40	C40	C45
Initial	Calculated	Calculated	Calculated
Pipe	Water sheet	Velocity head	Energy
	d	(V1^2)/(2*g)	E
	[m]	[m]	[m]
18	0.64	0.24	0.88

Table3 .34 Specific energy for actual flow [Author's own work]

Froude number

28The Froude number is calculated using the Froude equation:

$$NF = \frac{V}{\sqrt{g * H}} \quad (28)$$

C0	C37	C46	C47	C48
Initial	Calculated	Calculated	Calculated	Condition
Pipe	Velocity	Hydraulic depth	Froude number	
	V	H	NF	
	[m/s]	[m]	[Dimensionless]	Flow type
18	2.17	0.58	0.9	Subcritical

Table3 .35 Froude number [Author's own work]

Flow regime analysis

C0	C22	C23	C19	C49	C50	C51	C62	C63
Initial	Assumed	Assumed	Calculated	Calculated	Calculated	Calculated	Calculated	Calculated
Pipe	Nominal Diameter		Flow Rate	Flow ratio	Critical head	Critical head	Critical area	Critical velocity
			Design	ec	Yc	θ	Ac	Vc
	[m]	[in]	[L/s]	Dimensionless	[m]	[°]	[m ²]	[m/s]
16	36	0.91	1065.2	0.19	0.61	3.83	0.46	0.47

Table3 .36 Flow regime analysis [Author's own work]

Flow ratio, Critical chord, Critical angle, Critical area, Critical velocity

The flow ratio is calculated using equation (29); from this, the critical chord length is determined using equation (30), while the critical angle is obtained using equation (31). Similarly, the critical area is calculated using equation (32) and the critical velocity is determined using equation (33).

$$\epsilon_c = \frac{Q_{Dis}^2 * 10^{-6}}{g * D_{Dis}^5} \tag{29}$$

$$y_c = D_{Ad} * (1 + 13.6 * \epsilon_c^{-2.1135} - 13 * \epsilon_c^{-2.1})^{-0.1156} \tag{30}$$

$$\theta_c = 2 * ArcCos\left(1 - \frac{2 * y_c}{D_{Dis}}\right) \tag{31}$$

$$A_c = \frac{(100 * D_{Dis})^2}{8} * (\theta_c - Sen(\theta_c)) \tag{32}$$

$$V_c = \frac{Q_{Dis}}{A_c} \tag{33}$$

Specific energy for supercritical flow

34 To calculate the specific energy for supercritical flow (E_c), the following equation was used:

$$E_c = y_c + \frac{V_c^2}{2 * g} \tag{34}$$

C0	C49	C63	C78
Initial	Calculated	Calculated	Calculated
Pipe	Critical tie rod	Critical velocity	Supercritical in elongated structures with a drop
	Y_c	V_c	Specific energy for supercritical flow E_c
	Dimensionless	[m/s]	[m]
18	0.61	2.38	0.88

Table3 .37 Specific energy for supercritical flow [Author’s own work]

Well diameter

The equation35 was used to calculate the well diameter:

$$D_{P_Dis} = \frac{D_{Ext_s}}{\cos\left(\frac{\alpha}{2}\right)} \tag{35}$$

C0	C64	C67	C68	C69
Initial	Calculated	Calculated	Standardized	Calculated
Pipe	Pipe diameter D_{p_Dis}	Minimum well diameter D_{p_min}	Pipe diameter according to NEC	Adopted well diameter
	[m]	[m]	[m]	[m]
18	0.9	0.3	0.9	1.4

Table3 .38 Well diameter [Own work]

Curvature radius

37 To calculate the radius of curvature (R_c), the following equation was used:

$$R_c = \frac{D_{P_Dis}}{2 * \tan\left(\frac{\alpha}{2}\right)} \tag{37}$$

C0	C69	C70
Initial	Calculated	Calculated
Pipe	Adopted borehole diameter	Bend radius rc
	[m]	[m]
18	1.4	4.67

Table 3.39 Radius of curvature [Own work]

Well drop

C0	C22	C23	C19	C19	C76	C77	C80
Initial	Assumed	Assumed	Calculated	Calculated	Calculated	Calculated	Calculated
Pipe	Nominal Diameter		Flow	Increase due to losses	Inlet factor Fe	Head coefficient kc	Well head Hc
			Design	Ep			
	[m]	[in]	[L/s]	[m]	[Dimensionless]	[Dimensionless]	[m]
18	36	0.91	1065.2	0.04	0.43	1.40	1.29

Table 3.40 Well drop [Author's own work]

Height increase

The equation 38 was used to calculate the height increase:

Inlet factor

To calculate the head factor, the equation 39 was used:

$$F_e = \frac{Q_{Dis} * 10^{-3}}{\sqrt{g * D_{Dis}^5}} \tag{39}$$

$$F_e = 0.43 \leq 0.62 \rightarrow \text{Entrada sumergida}$$

Well drop height for submerged intake

The well head height was calculated using the equation 40 :

$$H_c = k_c * (E_c + E_p) \tag{40}$$

Energy losses

C0	C40	C65	C66	C72	C73	C74	C81
Initial	Calculated	Calculated	Calculated	Coefficient	Calculated	Calculated	Calculated
Pipe	$(V1^2)/(2 * g)$	Transition coefficient k_t	Transition loss H_t	Angle change coefficient k_d	Angular velocity loss H_d	Absolute loss H_e	Head loss H_p
	[m]	[Dimensionless]	[m]	[Dimensionless]	[m]	[m]	[m]
18	0.27	Accelerated	0.002	0.05	0.012	0.014	0.65

Table3 .41 Energy losses [Author’s own work]

Transition loss, directional change loss, absolute loss, and head loss
 Hydraulic losses were calculated using the corresponding equations: transition loss was determined using equation (42), change-of-direction loss using equation (43), total head loss using equation (44), and head loss using equation (45).

$$\Delta H_t = k_t * |h_{v_s} - h_{v_a}| \tag{42}$$

$$\Delta H_d = k_d * \left(\frac{h_{v_s} + h_{v_a}}{2} \right) \tag{43}$$

$$\Delta H_e = \Delta H_t + \Delta H_d \tag{44}$$

Elevations and depths for subsequent sections

Energy level

The energy level (CE) refers to the energy level of the flow in a section of the piping system (equation(53), considering the head loss due to the slope (S) and the length of the section (L) equation54 :

$$CE_f = CE_i - S * L \tag{54}$$

C0	C5	C20	C90	C91	C92
Initial	Initial	Assumed	Calculated	Calculated	Calculated
Pipe	Length	Slope	Energy level		
	L_Pipe	S	From	A	Entry to the next section
	[m]	[%]	[m]	[m]	[m]
18	74	0.5	4.8	4.5	4.5

Table3 .42 Energy level [Author’s own work]

C0	C90	C91	C92
Initial	Calculated	Calculated	Calculated
Pipe	Energy rating		
	From	To	Entry to the next section
	[m]	[m]	[m]
17	5.4	4.8	4.8

Table 3.43 Energy level of the previous section [Author’s own work]

Batea elevation

The head (CB) represents the height of the bottom of the conduit or pipe in terms of total energy (equation(55)). On the other hand, considering the slope of the section and the specific energy of the flow, the final head is calculated using equation56 :

C0	C5	C20	C45	C90	C86	C87
Home	Initial	Assumed	Calculated	Calculated	Calculated	Calculated
Pipe	Length	Slope	Energy	Energy elevation	Trough elevation	
	L_Pipe	S	E	From	From	A
	[m]	[%]	[m]	[m]	[m]	[m]
18	74	0.5	0.88	4.8	3.9	3.6

Table3 .44 Bate height [Author’s own work]

$$CB_i = CE_i - E \tag{55}$$

$$CB_f = CB_i - S * L \tag{56}$$

Key dimension

The key elevation (CC) refers to the height of the pipe’s top surface above sea level, calculated by adding the pipe’s nominal diameter to the bench elevation (equation57). Additionally, considering the slope of the section and the specific energy of the flow, the final key elevation is calculated (equation(58) :

Table3 .45 Key elevation [Author’s own work]

$$CC_i = CB_i + D_{Dis} \tag{57}$$

$$CC_f = CC_i - S * L \tag{58}$$

C0	C5	C20	C22	C23	C86	C87	C84	C85
Home	Initial	Assumed	Assumed	Assumed	Calculated	Calculated	Calculated	Calculated
Pipe	Length	Slope	Commercial Diameter		Trough elevation		Key elevation	
	L_Pipe	S			From	To	From	To
	[m]	[%]	[m]	[in]	[m]	[m]	[m]	[m]
18	74	0.5	36	0.91	3.9	3.6	4.9	4.5

Water Level

The water depth (CL) is the level at which the water surface is located inside the pipe. It is calculated by adding the water depth (d) to the initial water depth, as shown in equation59 . On the other hand, considering the slope of the section and the specific energy of the flow, the final water depth is calculated using

$$CL_i = CB_i + d \tag{59}$$

$$CL_f = CL_i - S * L \tag{60}$$

equation60 :

C0	C5	C20	C40	C86	C87	C88	C89
Home	Initial	Assumed	Calculated	Calculated	Calculated	Calculated	Calculated
Pipe	Length	Slope	Water depth	Trough level		Water depth	
	L_Pipe	S	d	From	To	From	To
	[m]	[%]	[m]	[m]	[m]	[m]	[m]
18	74	0.5	0.64	3.9	3.6	4.6	4.3

Table3 .46 Water level [Author’s own compilation]

Key elevation depth

The depth of the reference level (PCC) represents the vertical distance between the ground level (CR) and the reference level (CC) of the pipe. Equations61 -62 :

$$PCC_i = CR_i - CC_i \tag{61}$$

$$PCC_f = CR_f - CC_f \tag{62}$$

C0	C82	C83	C84	C85	C93	C94
Initial	Calculated	Calculated	Calculated	Calculated	Calculated	Calculated
Piping	Ground level		Key elevation		Depth to key elevation	
	From	To	From	To	From	To
	[m]	[m]	[m]	[m]	[m]	[m]
18	6.8	6.4	4.9	4.5	1.94	1.87

3 Table.47 Key depth [Author’s own work]

Pipe bed depth

The backfill depth (PCb) represents the vertical distance between the ground level (CR) and the backfill level (CB) of the pipe. Equations63 -64 :

$$PCB_i = CR_i - CB_i \tag{63}$$

$$PCB_f = CR_f - CB_f \tag{64}$$

C0	C82	C83	C86	C87	C95	C96
Initial	Calculated	Calculated	Calculated	Calculated	Calculated	Calculated
Piping	Ground level		Formwork level		Depth to formwork level	
	From	To	From	To	From	To
	[m]	[m]	[m]	[m]	[m]	[m]
18	6.8	6.4	3.9	3.6	2.85	2.78

Table3 .48 Depth of the battens [Author's own work]

Results

The most relevant results for the 136 resulting pipes are shown below:

C0	C1	C2	C5	C20	C26	C35	C37	C42	C93	C94	C95	C96
Inicial	Inicial	Inicial	Inicial	Asumido	Asumido	Tabla	Calculado	Calculado	Calculado	Calculado	Calculado	Calculado
Tubería	Pozos		Longitud	Pendiente	Diámetro	H/D	Velocidad	Fuerza tractiva	Profundidad de cota clave		Profundidad de cota batea	
	Inicial	Final	[m]	[%]	[pulg]	[Adimen]	[m/s]	[Pa]	Inicial [m]	Final [m]	Inicial [m]	Final [m]
1	74	53	57	0.8	6	0.85	0.90	3.60	1.20	1.66	1.35	1.81
2	2	3	118	0.5	16	0.71	1.30	5.40	1.45	2.61	1.86	3.02
3	3	4	108	0.5	20	0.64	1.50	6.70	2.59	2.70	3.10	3.21
4	4	5	137	0.5	24	0.57	1.60	7.70	2.67	2.33	3.28	2.94
5	5	6	106	0.5	27	0.49	1.60	8.40	2.28	1.88	2.97	2.57
6	6	7	80	0.5	27	0.52	1.70	8.60	1.96	2.04	2.65	2.73
7	7	8	38	0.5	30	0.75	2.00	10.10	2.20	2.41	2.96	3.17
8	8	9	32	0.5	30	0.74	2.00	10.10	2.48	3.44	3.24	4.20
9	9	10	92	0.5	42	0.74	2.60	15.80	3.19	1.28	4.26	2.35
10	11	12	52	0.5	16	0.71	1.30	5.40	1.32	1.56	1.73	1.97
11	12	13	69	0.5	16	0.69	1.30	5.40	1.57	1.92	1.98	2.33
12	13	14	114	0.5	18	0.55	1.30	5.80	1.87	1.34	2.33	1.80
13	14	15	108	0.5	18	0.85	1.50	6.20	1.43	1.88	1.89	2.34
14	15	7	105	0.5	20	0.78	1.50	6.80	1.88	1.54	2.39	2.05
15	16	17	120	0.5	20	0.55	1.40	6.40	1.80	2.36	2.31	2.87
16	17	18	73	0.5	36	0.53	2.00	11.40	2.49	1.97	3.40	2.88
17	18	19	50	0.5	36	0.62	2.10	11.80	2.07	1.91	2.98	2.82

C0	C1	C2	C5	C20	C26	C35	C37	C42	C93	C94	C95	C96
Inicial	Inicial	Inicial	Inicial	Asumido	Asumido	Tabla	Calculado	Calculado	Calculado	Calculado	Calculado	Calculado
Tubería	Pozos		Longitud	Pendiente	Diámetro	H/D	Velocidad	Fuerza tractiva	Profundidad de cota clave		Profundidad de cota batea	
	Inicial	Final	[m]	[%]	[pulg]	[Adimen]	[m/s]	[Pa]	Inicial [m]	Final [m]	Inicial [m]	Final [m]
18	19	20	74	0.5	36	0.64	2.20	11.90	1.94	1.87	2.85	2.78
19	20	21	109	0.5	36	0.80	2.30	12.20	1.98	2.37	2.89	3.28
20	21	9	32	0.5	36	0.78	2.30	12.20	2.37	3.23	3.28	4.14
21	22	23	87	0.5	10	0.53	0.90	3.30	1.20	1.61	1.45	2.47
22	23	3	41	0.5	14	0.58	1.10	4.60	2.24	2.06	2.60	2.42
23	24	25	55	0.5	8	0.85	0.90	2.80	1.20	1.46	1.40	1.52
24	25	4	68	0.5	12	0.80	1.10	4.00	1.32	1.02	1.62	1.32
25	26	27	120	0.5	24	0.46	1.50	7.30	1.19	1.65	1.80	2.26
26	27	17	67	0.5	33	0.49	1.90	10.30	1.98	2.38	2.82	3.22
27	28	29	109	0.5	24	0.55	1.60	7.70	2.02	2.51	2.63	3.12
28	29	30	48	0.5	24	0.58	1.60	7.80	2.57	2.09	3.18	2.70
29	30	27	77	0.5	27	0.47	1.60	8.30	2.04	2.00	2.73	2.69
30	31	32	103	0.5	18	0.55	1.30	5.80	1.62	1.18	2.08	1.64
31	32	33	24	0.5	20	0.65	1.50	6.70	1.26	1.46	1.77	1.97
32	90	91	61	0.5	14	0.51	1.10	4.50	1.20	1.47	1.56	1.95
33	33	34	76	0.5	24	0.44	1.50	7.20	1.43	1.77	2.04	2.38
34	1	48	59	0.5	12	0.52	1.00	3.70	1.20	1.47	1.50	1.11

C0	C1	C2	C5	C20	C26	C35	C37	C42	C93	C94	C95	C96
Inicial	Inicial	Inicial	Inicial	Asumido	Asumido	Tabla	Calculado	Calculado	Calculado	Calculado	Calculado	Calculado
Tubería	Pozos		Longitud	Pendiente	Diámetro	H/D	Velocidad	Fuerza tractiva	Profundidad de cota clave		Profundidad de cota batea	
	Inicial	Final	[m]	[%]	[pulg]	[Adimen]	[m/s]	[Pa]	Inicial [m]	Final [m]	Inicial [m]	Final [m]
35	37	38	50	0.5	12	0.61	1.00	3.90	1.20	1.42	1.50	2.14
36	36	81	66	0.5	14	0.54	1.10	4.50	0.80	1.10	1.16	1.34
37	38	39	92	0.5	12	0.65	1.00	3.90	1.86	2.51	2.16	2.81
38	39	40	66	0.5	27	0.57	1.70	8.80	3.42	3.46	4.11	4.15
39	40	41	48	0.5	30	0.48	1.70	9.20	3.39	3.29	4.15	4.05
40	76	20	139	0.5	10	0.70	0.90	3.30	1.62	2.25	1.87	1.99
41	42	43	80	0.5	10	0.65	0.90	3.30	2.82	3.18	3.07	3.10
42	43	44	16	0.5	14	0.55	1.10	4.50	2.82	2.59	3.18	2.95
43	44	45	65	0.5	14	0.68	1.20	4.70	2.64	2.48	3.00	2.84
44	45	46	50	0.5	16	0.73	1.30	5.40	2.50	2.64	2.91	3.05
45	46	47	75	0.5	36	0.58	2.10	11.60	2.86	1.35	3.77	2.26
46	48	49	48	0.5	14	0.69	1.20	4.70	1.42	1.43	1.78	1.79
47	49	50	115	0.5	16	0.53	1.20	5.10	1.38	1.06	1.79	1.47
48	50	51	109	0.5	20	0.54	1.40	6.40	1.16	1.37	1.67	1.88
49	51	46	113	0.5	36	0.51	2.00	11.30	2.91	2.80	3.82	3.71
50	52	50	163	0.5	10	0.77	1.00	3.30	1.14	1.20	1.39	1.45
51	53	54	110	0.5	10	0.47	0.90	3.30	1.58	0.69	1.83	0.94

C0	C1	C2	C5	C20	C26	C35	C37	C42	C93	C94	C95	C96
Inicial	Inicial	Inicial	Inicial	Asumido	Asumido	Tabla	Calculado	Calculado	Calculado	Calculado	Calculado	Calculado
Tubería	Pozos		Longitud	Pendiente	Diámetro	H/D	Velocidad	Fuerza tractiva	Profundidad de cota clave		Profundidad de cota batea	
	Inicial	Final	[m]	[%]	[pulg]	[Adimen]	[m/s]	[Pa]	Inicial [m]	Final [m]	Inicial [m]	Final [m]
52	54	55	114	0.5	14	0.47	1.10	4.30	0.67	0.60	1.03	0.96
53	80	71	80	0.5	8	0.80	0.90	2.90	1.20	1.58	1.40	1.63
54	68	69	109	0.5	24	0.64	1.70	8.00	2.05	2.30	2.66	2.91
55	57	45	68	0.5	8	0.73	0.90	2.90	2.00	2.34	2.20	2.14
56	77	58	106	0.5	30	0.47	1.70	9.20	3.33	3.81	4.09	4.57
57	59	23	71	0.5	10	0.56	0.90	3.20	1.20	1.52	1.45	1.77
58	60	61	39	0.7	6	0.85	0.90	3.10	1.20	1.47	1.35	1.35
59	61	62	108	0.5	10	0.58	0.90	3.20	1.15	1.22	1.40	1.47
60	62	63	111	0.5	12	0.65	1.00	3.90	1.23	1.17	1.53	1.47
61	63	55	70	0.5	14	0.62	1.20	4.70	1.18	1.34	1.54	1.70
62	55	56	110	0.5	24	0.37	1.40	6.60	1.19	1.65	1.80	2.26
63	65	43	65	0.7	8	0.47	0.90	3.50	1.73	2.15	1.93	2.29
64	66	67	105	0.5	12	0.64	1.00	3.90	0.78	1.25	1.08	2.07
65	67	68	110	0.5	14	0.60	1.10	4.60	1.76	1.97	2.12	2.33
66	64	56	71	0.5	27	0.59	1.80	8.80	2.64	2.94	3.33	3.63
67	69	64	70	0.5	24	0.82	1.70	8.20	2.42	2.72	3.03	3.33
68	70	67	68	1.1	6	0.40	0.90	4.10	1.10	1.84	1.25	1.86

C0	C1	C2	C5	C20	C26	C35	C37	C42	C93	C94	C95	C96
Inicial	Inicial	Inicial	Inicial	Asumido	Asumido	Tabla	Calculado	Calculado	Calculado	Calculado	Calculado	Calculado
Tubería	Pozos		Longitud	Pendiente	Diámetro	H/D	Velocidad	Fuerza tractiva	Profundidad de cota clave		Profundidad de cota batea	
	Inicial	Final	[m]	[%]	[pulg]	[Adimen]	[m/s]	[Pa]	Inicial [m]	Final [m]	Inicial [m]	Final [m]
69	71	72	160	0.5	10	0.49	0.90	3.20	1.39	1.73	1.64	1.98
70	72	73	60	0.5	24	0.45	1.50	7.20	1.66	1.79	2.27	2.40
71	73	68	30	0.5	24	0.48	1.50	7.40	1.82	1.90	2.43	2.51
72	81	75	56	0.5	18	0.75	1.40	6.10	1.05	1.45	1.51	1.91
73	41	77	68	0.5	30	0.47	1.70	9.20	3.36	3.27	4.12	4.03
74	58	96	46	0.5	30	0.53	1.80	9.50	3.88	4.09	4.64	4.85
75	78	79	53	0.5	8	0.73	0.90	2.90	1.20	1.47	1.40	1.70
76	79	40	104	0.5	10	0.67	0.90	3.30	1.50	1.97	1.75	2.22
77	56	51	71	0.5	33	0.50	1.90	10.40	2.83	2.92	3.67	3.76
78	75	72	23	0.5	20	0.60	1.40	6.50	1.41	1.56	1.92	2.07
79	82	84	75	0.5	10	0.68	0.90	3.30	0.45	0.79	0.70	1.04
80	83	35	108	0.5	10	0.85	1.00	3.40	1.20	1.69	1.45	1.96
81	84	32	42	0.5	12	0.53	1.00	3.80	0.76	1.07	1.06	1.37
82	85	86	121	0.5	27	0.48	1.60	8.40	2.56	2.49	3.25	3.18
83	87	18	150	0.5	16	0.70	1.30	5.40	0.97	1.82	1.38	2.23
84	88	89	110	0.5	14	0.58	1.10	4.60	1.68	1.39	2.04	1.75
85	89	87	79	0.5	16	0.57	1.20	5.20	1.38	0.92	1.79	1.33

C0	C1	C2	C5	C20	C26	C35	C37	C42	C93	C94	C95	C96
Inicial	Inicial	Inicial	Inicial	Asumido	Asumido	Tabla	Calculado	Calculado	Calculado	Calculado	Calculado	Calculado
Tubería	Pozos		Longitud	Pendiente	Diámetro	H/D	Velocidad	Fuerza tractiva	Profundidad de cota clave		Profundidad de cota batea	
	Inicial	Final	[m]	[%]	[pulg]	[Adimen]	[m/s]	[Pa]	Inicial [m]	Final [m]	Inicial [m]	Final [m]
86	34	35	71	0.5	27	0.41	1.50	7.80	1.69	1.83	2.38	2.52
87	35	85	119	0.5	27	0.48	1.60	8.40	1.93	2.55	2.62	3.24
88	91	88	69	0.5	14	0.53	1.10	4.50	1.62	1.64	1.98	2.00
89	93	48	55	0.6	8	0.48	0.90	3.50	1.03	1.39	1.23	1.59
90	86	39	74	0.5	27	0.53	1.70	8.60	2.59	3.38	3.28	4.07
91	92	93	21	0.7	6	0.78	0.90	3.20	1.11	1.25	1.26	1.23
92	94	95	79	0.5	10	0.65	0.90	3.30	1.01	1.36	1.26	1.97
93	95	52	57	0.5	10	0.82	1.00	3.40	1.75	1.14	2.00	1.39
94	96	97	51	0.5	30	0.53	1.80	9.50	4.18	3.18	4.94	3.94
95	98	99	30	0.5	10	0.53	0.90	3.30	1.20	1.34	1.45	1.05
96	99	100	105	0.5	10	0.53	0.90	3.10	1.34	1.54	1.59	1.79
97	100	31	12	0.5	10	0.53	0.90	3.10	1.55	1.61	1.80	1.86
98	101	99	56	3.1	4	0.23	0.90	5.40	0.15	1.87	0.25	1.46
99	102	103	63	0.7	6	0.85	0.90	3.10	1.20	1.64	1.35	1.43
100	103	104	75	0.5	8	0.85	0.90	2.90	1.27	1.22	1.47	1.42
101	104	31	83	0.5	12	0.53	1.00	3.70	1.17	1.40	1.47	1.70
102	105	106	64	0.7	8	0.43	0.90	3.60	0.95	1.39	1.15	1.60

Table 3.49 Results for pipes 1 through 136 [Author's own work]

C0	C1	C2	C5	C20	C26	C35	C37	C42	C93	C94	C95	C96
Inicial	Inicial	Inicial	Inicial	Asumido	Asumido	Tabla	Calculado	Calculado	Calculado	Calculado	Calculado	Calculado
Tubería	Pozos		Longitud	Pendiente	Diámetro	H/D	Velocidad	Fuerza tractiva	Profundidad de cota clave		Profundidad de cota batea	
	Inicial	Final	[m]	[%]	[pulg]	[Adimen]	[m/s]	[Pa]	Inicial [m]	Final [m]	Inicial [m]	Final [m]
103	106	107	71	0.5	14	0.67	1.20	4.70	1.46	1.66	1.82	2.02
104	107	108	69	0.5	16	0.65	1.30	5.40	1.66	1.53	2.07	1.94
105	108	109	78	0.5	18	0.55	1.30	5.80	1.49	1.40	1.95	1.86
106	109	139	81	0.5	18	0.70	1.40	6.10	1.49	1.86	1.95	2.32
107	139	28	40	0.5	20	0.85	1.60	6.90	1.90	2.08	2.41	2.59
108	110	106	75	0.5	12	0.49	0.90	3.70	1.05	1.39	1.35	1.69
109	111	112	77	0.5	10	0.54	0.90	3.10	1.20	1.55	1.45	1.62
110	112	113	63	0.5	10	0.80	1.00	3.30	1.42	1.42	1.67	1.67
111	113	114	71	0.5	12	0.63	1.00	3.90	1.39	1.32	1.69	1.62
112	114	115	70	0.5	14	0.71	1.20	4.80	1.34	1.51	1.70	1.87
113	115	116	69	0.5	16	0.56	1.20	5.20	1.46	1.61	1.87	2.02
114	116	121	75	0.5	16	0.67	1.30	5.40	1.68	1.18	2.09	1.59
115	121	26	16	0.5	24	0.47	1.50	7.30	1.06	1.13	1.67	1.74
116	117	118	63	0.5	8	0.61	0.90	3.10	1.20	1.54	1.40	1.44
117	118	119	70	0.5	12	0.62	1.00	3.90	1.23	1.04	1.53	1.34
118	119	120	70	0.5	14	0.75	1.20	4.80	1.07	0.85	1.43	1.21
119	120	121	66	0.5	16	0.60	1.20	5.30	0.80	1.08	1.21	1.49

C0	C1	C2	C5	C20	C26	C35	C37	C42	C93	C94	C95	C96
Inicial	Inicial	Inicial	Inicial	Asumido	Asumido	Tabla	Calculado	Calculado	Calculado	Calculado	Calculado	Calculado
Tubería	Pozos		Longitud	Pendiente	Diámetro	H/D	Velocidad	Fuerza tractiva	Profundidad de cota clave		Profundidad de cota batea	
	Inicial	Final	[m]	[%]	[pulg]	[Adimen]	[m/s]	[Pa]	Inicial [m]	Final [m]	Inicial [m]	Final [m]
120	122	123	98	1.2	6	0.36	0.90	4.20	0.50	1.67	0.65	1.53
121	123	124	46	0.5	10	0.49	0.90	3.20	1.33	1.25	1.58	1.50
122	124	125	70	0.5	12	0.52	1.00	3.70	1.25	1.04	1.55	1.34
123	125	126	70	0.5	16	0.62	1.30	5.30	1.07	1.38	1.48	1.79
124	126	127	67	0.5	18	0.53	1.30	5.70	1.34	1.64	1.80	2.10
125	127	16	19	0.5	18	0.60	1.30	5.90	1.70	1.79	2.16	2.25
126	128	129	69	0.5	10	0.58	0.90	3.20	1.20	1.51	1.45	0.96
127	129	130	70	0.5	12	0.53	1.00	3.70	0.70	0.81	1.00	1.11
128	130	131	66	0.5	12	0.74	1.10	4.00	0.87	1.16	1.17	1.46
129	131	11	24	0.5	14	0.56	1.10	4.60	1.14	1.25	1.50	1.61
130	132	133	43	0.5	12	0.60	1.00	3.90	0.75	0.94	1.05	1.24
131	133	134	65	0.5	12	0.58	1.00	3.80	0.95	1.24	1.25	1.54
132	134	2	29	0.5	12	0.75	1.10	4.00	1.29	1.42	1.59	1.72
133	135	2	11	0.5	8	0.63	0.90	3.10	1.20	1.26	1.40	1.46
134	136	134	52	1.1	6	0.38	0.90	4.10	0.65	1.24	0.80	1.39
135	137	138	68	0.5	12	0.60	1.00	3.90	1.20	1.50	1.50	1.58
136	138	139	76	0.5	14	0.52	1.10	4.50	1.25	1.58	1.61	1.94

To ensure the project’s success and proper implementation, it is essential to conduct additional studies to supplement the information used during the design phase. Among these, detailed studies of soil characteristics in Puerto Villamil are particularly important, as local conditions could differ significantly from those assumed in the project. Likewise, it is essential to develop IDF curves specific to the area, as those from Santa Cruz Island were used, which introduces uncertainty into the design’s hydrological parameters.

The budget and schedule presented in this project are for reference only and must be adjusted during the execution phase. It is recommended to consider additional factors such as the logistics associated with transporting materials to the island, the availability of skilled labor, and other indirect costs that may arise. It is also crucial to include a detailed analysis of environmental aspects, such as impact mitigation during construction and operation, as well as the environmental permits necessary to comply with current regulations and protect the island’s unique biodiversity.

Furthermore, it is suggested to plan for construction waste management and the restoration of affected areas to minimize the impact on local ecosystems.

Coordination with local and national entities to secure funding, permits, and technical support will be essential to ensure the project's long-term viability. Finally, it is advisable to develop a continuous monitoring system that allows for the evaluation of the stormwater system's performance and the adjustment of its operation according to changing environmental conditions. This monitoring, along with the updating of hydrological and geotechnical data, will contribute to maintaining the system's sustainability and effectiveness over time.

CONCLUSIONS

An analysis of the proposed system was conducted, achieving a 38% reduction in total runoff volume, which allowed for a reduction in excavation depths and the required pipe diameters. This optimized design resulted in the installation of 136 pipes, 136 manholes, and 3 outfalls, of which 4 manholes will require specific drop structures for proper operation.

The system layout was modeled using the open-source software SWMM, where it was verified that it meets the pipe capacity, velocities, and head required for proper operation. The average values obtained for these parameters are a 0.60 m H/D ratio, a 1.3 m/s velocity, and a 5.7 Pa head, thus ensuring that the design meets hydraulic efficiency standards.

The total area designated for Sustainable Urban Drainage Systems (SUDs) covers 2.12 hectares, within which solutions such as permeable pavements, structural tree pits, rain gardens, and green swales were implemented, contributing to environmental sustainability and efficient stormwater management.

The total project budget amounts to \$3,935,474.73, distributed as follows: 39% allocated to the purchase and installation of pipes, 30% allocated to the development and implementation of SUDs, and 25% allocated to earthwork activities. This breakdown demonstrates a balanced approach between traditional infrastructure and sustainable solutions.

REFERENCES

- Y. Xiao and J. Vasconcelos, "Urban stormwater modeling using rainfall-runoff relationships: Revisiting the rational method in modern contexts," *Journal of Hydrologic Engineering*, vol. 28, no. 5, pp. 1–12, 2023, doi: 10.1061/JHYEFF.HY.0002345
- A. R. Diogo and J. S. do Carmo, "Urban drainage design and the rational method: A revisit," *Journal of Hydrology and Hydromechanics*, vol. 67, no. 3, pp. 282–291, 2019, doi: 10.2478/johh-2019-0026

- N. S. Grigg, "Stormwater management: An integrated approach to support healthy, livable, and ecological cities," *Urban Science*, vol. 8, no. 3, p. 89, 2024, doi: 10.3390/urbansci8030089
- J. Wang, Y. Zhao, and C. Liu, "Integrated sponge city planning and stormwater management in urban China," *Sustainability (Switzerland)*, vol. 16, no. 4, p. 2061, 2024, doi: 10.3390/su16042061
- Y. Zhang, W. Zhao, X. Chen, C. Jun, J. Hao, X. Tang, and J. Zhai, "Assessment on the effectiveness of urban stormwater management," *Water (Switzerland)*, vol. 13, no. 1, pp. 1–15, 2021, doi: 10.3390/w13010004
- S. Bouarafa, L. Lassabatere, G. Lipeme-Kouyi and R. Angulo-Jaramillo, "Hydrodynamic characterization of Sustainable Urban Drainage Systems (SuDS) using Beerkan infiltration experiments," *Water (Switzerland)*, vol. 11, no. 4, p. 606, 2019, doi: 10.3390/w11040660
- F. Chapa, M. Pérez, and J. Hack, "Experimenting with the transition to sustainable urban drainage systems—identifying constraints and unintended processes in a tropical, highly urbanized watershed," *Water (Switzerland)*, vol. 12, no. 12, p. 3544, 2020, doi: 10.3390/w12123554
- M. Hu, X. Zhang, Y. L. Siu, Y. Li, K. Tanaka, H. Yang, and Y. Xu, "Flood mitigation by permeable pavements in Chinese sponge city construction," *Water (Switzerland)*, vol. 10, no. 2, p. 173, 2018, doi: 10.3390/w10020172
- M. Jeon, H. B. Guerra, H. Choi, D. Kwon, H. Kim and L. H. Kim, "Stormwater runoff treatment using rain gardens: Performance monitoring and development of deep learning-based water quality prediction models," *Water (Switzerland)*, vol. 13, no. 24, p. 3488, 2021, doi: 10.3390/w13243488
- F. Y. Lim, T. H. Neo, H. Guo, S. Z. Goh, S. L. Ong, J. Hu, B. C. Y. Lee, G. S. Ong, and C. X. Liou, "Pilot and field studies of modular bioretention tree system with *Talipariti tiliaceum* and engineered soil filter media in the tropics," *Water (Switzerland)*, vol. 13, no. 13, p. 1817, 2021, doi: 10.3390/w13131817
- M. Sulis, T. Zhang, and D. Ryu, "Economic performance of sustainable urban drainage systems: Long-term benefits under climate uncertainty," *Water Resources Management*, vol. 38, no. 2, pp. 214–228, 2024, doi: 10.1007/s11269-023-03527-1
- T. H. S. Francisco, O. V. C. Menezes, A. L. A. Guedes, G. Maquera, D. C. V. Neto, O. C. Longo, C. K. Chinelli, and C. A. P. Soares, "The main challenges for improving urban drainage systems from the perspective of Brazilian

- professionals,” *Infrastructures*, vol. 8, no. 1, p. 5, 2023, doi: 10.3390/infrastructures8010005
- M. Ragazzi, R. Catellani, E. C. Rada, V. Torretta, and X. Salazar-Valenzuela, “Management of urban wastewater on one of the Galapagos Islands,” *Sustainability (Switzerland)*, vol. 8, no. 3, p. 208, 2016, doi: 10.3390/su8030208
- C. Allende-Prieto, B. I. Méndez-Fernández, L. A. Sañudo-Fontaneda, and S. M. Charlesworth, “Development of a geospatial data-based methodology for stormwater management in urban areas using freely-available software,” *International Journal of Environmental Research and Public Health*, vol. 15, no. 8, p. 1703, 2018, doi: 10.3390/ijerph15081703
- G. Senes, P. S. Ferrario, G. Cirone, N. Fumagalli, P. Frattini, G. Sacchi and G. Valè, “Nature-based solutions for stormwater management: Creation of a green infrastructure suitability map as a tool for land-use planning,” *Sustainability (Switzerland)*, vol. 13, no. 11, p. 6124, 2021, doi: 10.3390/su13116124
- Y. Dong, Y. Han, X. Han, Y. Chen, and Y. Zhai, “Sewage vertical infiltration introduced polygenic multipollutants into groundwater,” *Water (Switzerland)*, vol. 16, no. 16, p. 2305, 2024, doi: 10.3390/w16162305
- S. R. Yang, X. R. Chen, H. X. Huang, and H. F. Yeh, “Innovation in water management: Designing a recyclable water resource system with permeable pavement,” *Water (Switzerland)*, vol. 16, no. 15, p. 2109, 2024, doi: 10.3390/w16152109
- A. Alzueta Pérez, *Climate and Biodiversity of the Galápagos Islands*. Zaragoza, Spain: University of Zaragoza Press, 2014, ISBN 978-84-16723-14-3
- M. Maestro, M. L. Pérez-Cayeiro, H. Reyes, and J. A. Chica-Ruiz, “Ecology and Volcanic Dynamics of Isabela Island, Galápagos,” *Journal of Environmental Sciences*, vol. 42, no. 1, pp. 15–29, 2024, doi: 10.15359/rca.42-1.2
- Isabela Municipal Decentralized Autonomous Government, *Isabela Development and Land Use Plan 2023–2035*, Isabela, Ecuador, 2023
- EMAAP-Q, *Design Standards for Sewer Systems*, Quito, Ecuador, 2009
- R. A. López Cualla, *Design Elements for Water Supply and Sewer Systems*, Bogotá, Colombia: Colombian School of Engineering, 2nd ed., 2003, ISBN 978-9701504024

INEN, Standards for the Study and Design of Drinking Water and Wastewater Disposal Systems for Populations Larger than 1,000 Inhabitants, Quito, Ecuador, 1997